Mon. Not. R. Astron. Soc. **000**, 000–000 (0000) Printed 1 February 2008 (MN LATEX style file v1.4)

The 2dF BL Lac Survey

D. Londish[1,2], S.M. Croom[2], B.J. Boyle[2], T. Shanks[3], P.J. Outram[3], E.M. Sadler[1], N.S. Loaring[4], R.J. Smith[5], L. Miller[4], P.F.L. Maxted[6,7]

[1] *University of Sydney, School of Physics, Sydney NSW 2006, Australia*
[2] *Anglo-Australian Observatory, PO Box 296, Epping, NSW 1710, Australia*
[3] *Department of Physics, University of Durham, South Road, Durham, DH1 3LE, UK*
[4] *Department of Physics, Oxford University, 1 Keble Road, Oxford, OX1 3RH, UK*
[5] *Liverpool John Moores University, Twelve Quays House, Egerton Wharf, Birkenhead, CH41 1LD, UK*
[6] *Department of Physics & Astronomy, University of Southampton, Highfield, Southampton SO17 1BJ, UK*
[7] *Department of Physics, Keele University, Staffordshire, ST5 5BG, UK*

arXiv:astro-ph/0202386v1 21 Feb 2002

1 February 2008

ABSTRACT

We have optically identified a sample of 56 featureless continuum objects without significant proper motion from the 2dF QSO Redshift Survey (2QZ). The steep number–magnitude relation of the sample, $n(b_{\rm J}) \propto 10^{0.7b_{\rm J}}$, is similar to that derived for QSOs in the 2QZ and inconsistent with any population of Galactic objects. Follow up high resolution, high signal-to-noise, spectroscopy of five randomly selected objects confirms the featureless nature of these sources. Assuming the objects in the sample to be largely featureless AGN, and using the QSO evolution model derived for the 2QZ, we predict the median redshift of the sample to be $z = 1.1$. This model also reproduces the observed number-magnitude relation of the sample using a renormalisation of the QSO luminosity function, $\Phi^* = \Phi^*_{\rm QSO}/66 \simeq 1.65 \times 10^{-8}\,{\rm mag}^{-1}{\rm Mpc}^{-3}$. Only ∼20 per cent of the objects have a radio flux density of $S_{1.4} > 3\,$mJy, and further VLA observations at 8.4 GHz place a 5σ limit of $S_{8.4} < 0.2$mJy on the bulk of the sample. We postulate that these objects could form a population of radio-weak AGN with weak or absent emission lines, whose optical spectra are indistinguishable from those of BL Lac objects.

Key words: BL Lac objects – galaxies: active – quasars: general

1 INTRODUCTION

Over the last decade research into the nature of BL Lac objects has greatly increased our understanding of this enigmatic and intrinsically rare class of active galactic nuclei (AGN). Nevertheless, small number statistics and inhomogeneous samples have left many key questions unanswered. In particular the evolutionary behaviour of the BL Lac population is poorly known, and from recent survey results (e.g. Padovani & Giommi 1995; Bade et al. 1998; Rector et al. 2000) appears inconsistent with trends observed in the population of AGN as a whole.

BL Lacs are thought to be dominated by emission from a non-thermal, relativistic jet emanating from the galaxy's core. Their optical spectra are thus characterised by an absence of prominent emission or absorption features, making them difficult to target in optical surveys. Initial detection is therefore usually at either X-ray or radio frequencies, with subsequent optical follow-up. Not surprisingly, surveys conducted at these different frequencies find differing classes of objects, with the BL Lacs selected in radio surveys (e.g. the 1 Jy BL Lac Sample, Stickel et al. 1991) being predominantly the radio-loud or low energy peaked variety (LBLs), whilst X-ray selected samples are characterised by a population of less luminous (optically and at radio frequencies), X-ray dominant, high energy peaked BL Lacs (HBLs) (e.g. the EMSS BL Lac Sample, Morris et al. 1991).

Although deeper, multiwavelength surveys have overcome some of the problems of selection bias and high flux limits (for example, the *ROSAT* All Sky Survey-Greenbank BL Lac Sample (Laurent-Muehleisen et al. 1999), revealing a new population of IBLs – BL Lacs with properties intermediate between those of LBLs and HBLs), greater coverage of objects at the very faint end of the luminosity scale is still necessary if the question of BL Lac evolution is to be addressed satisfactorily. The current understanding is that, while LBLs and IBLs exhibit mildly positive or no evolution (Rector & Stocke 2001, Laurent-Muehleisen et al. 1999) the HBLs appear to evolve negatively, that is they were either less numerous or less luminous in the past (Wolter et al. 1994, Rector et al. 2000). This is in direct contrast to the

© 0000 RAS

trend of strong, positive evolution exhibited by other classes of AGN.

Estimating the relative numbers of LBLs and HBLs is similarly hampered by survey flux limits and selection biases (Urry & Padovani 1995; Fossati 2001). Furthermore finding low luminosity BL Lac objects at higher redshifts is likely to be difficult at X-ray frequencies, given that these objects are also characterised by a lower Doppler factor, $\delta^{\star}$, and hence lower ν_{peak} (Giommi et al. 2001). Thus at the emitted frequency the flux may well fall below the survey flux limit, and as a consequence omission of these fainter, extreme HBLs would result in an artificial flattening of the number–flux (N–S) relation for this class of BL Lac.

Clearly selection at optical wavelengths (below ν_{peak}) would overcome some of the bias in estimating numbers of LBLs and HBLs (Urry & Padovani 1995). Furthermore, an optically flux-limited survey essentially places no upper or lower limits on the radio and X-ray fluxes of objects in the sample; the difficulty has always been the amount of telescope time required to assemble such a sample. Recently, however, an opportunity has arisen to select BL Lac candidates primarily from optical observations using the 2dF QSO Redshift Survey (2QZ, Croom et al. 2001). On completion the 2QZ will contain almost 50000 spectra of UBR colour-selected stellar objects at magnitudes $18.25 < b_{\rm J} \leq 20.85$, of which approximately 25000 will be QSOs.

In this paper we present an initial analysis of 56 objects with featureless continuum spectra and no significant proper motion, selected from the 2QZ catalogue as at July 2001. Our procedure for the selection of BL Lac candidates from this catalogue is described in section 2; in section 3 we present details of the radio and optical observations and derive in section 4 the number-magnitude relation for this sample of candidate BL Lac objects. A discussion of our findings follows in Section 5.

2 THE 2DF BL LAC SURVEY

2.1 The 2QZ catalogue

The 2QZ is a large spectroscopic survey of QSO candidates which, when complete, will result in the spectroscopic identification of a catalogue of ∼25000 QSOs, more than twenty times larger than any previous such catalogue. The survey has been made possible by the 2-degree field (2dF), 400-fibre multi-object spectrograph at the Anglo-Australian Telescope (Lewis et al. 2001). The survey area covers a total of 740 deg^2, made up of two 75^o x 5^o strips, one centered on $\delta = -30^{\circ}$ with RA range 21^h40 to 3^h15 (southern strip) and the other centered on $\delta = 0^o$ with RA range 9^h50 to 14^h50 (equatorial strip). QSO candidates were selected from APM measurements of UK Schmidt U, J and R plates/films on the basis of their $u - b_{\rm J}/b_{\rm J} - r$ colours and $18.25 < b_{\rm J} \leq 20.85$. A detailed description of the creation of the input catalogue is given in Smith et al. (2002). The key features of the selection criteria are that objects satisfy either $u' - b_{\rm J} \leq -0.36$ or $u' - b_{\rm J} < 0.12 - 0.8(b_{\rm J} - r)$ or $b_{\rm J} - r < 0.05$, where $u' = u - 0.24$. Further information is available at http://www.2dfquasar.org.

2.2 Selection of continuum sources

The first 2dF observations for the QSO survey were made in September 1997 and by July 2001 the catalogue contained 40736 objects, of which 50.5 per cent are QSOs. This version of the catalogue, representing an intermediate stage between the 10k catalogue (Croom et al. 2001) and final catalogues, was used as the basis for selecting the BL Lac candidates in the current sample. The total area covered by this catalogue is 613 deg^2.

The spectroscopic data from 2dF were initially reduced using the 2dF pipeline reduction system (Bailey et al. 2002). Classification and redshift estimation for the QSOs was carried out using a specially written AUTOZ code (Miller et al. in preparation) based on a χ^2 fit to stellar/QSO templates. All AUTOZ classifications were checked and double-checked by independent 2QZ team members to ensure a high-level of catalogue reliability (97 per cent, see Croom et al. 2001). With the express purpose of identifying objects with featureless spectra, all spectra satisfying $18.25 < b_{\rm J} \leq 20.00$ and with a measured signal-to-noise ratio (SNR) of ≥ 10.0 were visually re-examined (see section 2.3). Fainter objects satisfying the SNR criterion were not included in the analysis because it would be difficult to obtain follow-up spectroscopic observations at higher resolution/signal-to-noise. A number of fields were observed during periods of significant moonlight. In some cases this moonlight caused excess scattered light in the 2dF spectrographs which was not completely removed by the data reduction process. This produced artificially high, featureless continuum levels for some objects observed in those fields. Consequently we removed all fields with strong moonlight, determined from sky counts in that field. With the removal of these fields the total survey area became 544 deg^2.

2.3 Visual classification

From this area we selected for visual re-examination 6772 objects satisfying the above selection criteria. Approximately 15 per cent of the objects in the 2QZ have two or more spectra obtained at different times during survey observations. Different spectra of the same objects were also inspected and classified independently.

Objects with featureless continua are inherently difficult to classify. For consistency, we adopted the standard operational definition of a BL Lac as an extragalactic object with no emission lines greater than W_λ =5Å and Ca II H&K break contrast of less than 0.25 (Stocke et al. 1990). We took great care to remove all Galactic subdwarfs with weak absorption lines (Ca II H&K, Balmer series, He I, He II, Mg H) and also QSOs with emission lines.

Provided they met these criteria, we also included objects with non-stellar absorption lines to avoid bias against high redshift objects with intervening absorbers. We also included objects with extremely broad (> 200Å) and unidentifiable emission humps or dips in the continuum. This was to avoid bias against lineless QSOs with broad absorption line systems which would also fulfil the BL Lac classifica-

* $\delta = (\Gamma(1 - \beta cos\theta))^{-1}$, where $\Gamma = (1 - \beta^2)^{-1/2}$, θ is the angle to the line of sight and βc is the bulk velocity of the jet; when $\theta = 1/\Gamma, \delta = \Gamma$

tion criteria. Care was taken to avoid selecting peculiar low-ionisation broad absorption line (BAL) QSOs (Becker et al. 1997) under this latter criterion. We attempted to minimise any subjectivity in this visual classification scheme by using three independent examiners (DL, SMC and BJB). To be accepted as a continuum source, an object spectrum has to be classified as such by at least two people independently. Two of the people who carried out the visual inspection (SMC and BJB) have also examined visually all 40000 spectra observed to date (August 2001) in the 2QZ. Selection of continuum objects was therefore made by those with significant experience of the visual appearance of a wide range of optical QSO spectra. While the 'continuum' spectra selected here may simply represent the objects in the extreme tail of the QSO emission line equivalent width distribution, they are markedly different in spectral appearance from the 20000 QSOs identified to date in the 2QZ.

Based on these criteria, 74 objects out of the 6772 initially selected to have high signal-to-noise spectra were classified as having continuum spectra.

2.4 Removing contamination by white dwarfs

Although the identifying feature of a BL Lac object at optical wavelengths is an absence of features, it clearly does not follow that all featureless continuum objects are BL Lacs. The most likely non-AGN class of objects which could be confused with a BL Lac on the basis of their optical spectra are continuum DC white dwarfs (e.g. Wesemael et al 1993). One feature which can distinguish between AGN and DC white dwarfs is a measurement of proper motion. We would expect DC white dwarfs to exhibit a detectable proper motion over the typical period between the UKST J and R photographic plates used to create the 2QZ input catalogue. Based on the McCook & Sion (1999) catalogue DC white dwarfs exhibit a range in absolute magnitude $12 < M_B < 16$ with a median $M_B = 14$. Even if we assume that the colour selection would have biased any selection of DC white dwarfs towards the brightest absolute magnitudes ($M_B \sim 12$), this corresponds to a distance of 275 pc at $B = 19.2$, the median magnitude of our sample. With typical transverse velocities observed in the range $30 - 80$ km s^{-1} (Sion et al. 1988), at this distance DC white dwarfs would exhibit proper motions $\sim 23 - 60$ mas yr^{-1}.

We used the SuperCOSMOS Sky Survey† to search for proper motions in our sample based on the positions measured from the UKST J and R sky survey plates. Given the typical astrometric accuracy obtainable from the J and R photographic plates (~ 0.10 arcsec in each co-ordinate) and the typical mean epoch separation (16 years for fields in the southern strip, and 11 years for 8 fields in the equatorial strip), we are sensitive at the 3σ level to proper motions with 30 mas yr^{-1}. This should be sufficient to detect the bulk of the DC white dwarf population.

Of the 74 objects originally selected, 18 exhibited proper motions detectable at $\geq 3\sigma$. Of these 18 objects, the typical apparent proper motions ranged from 30 to 100 mas yr^{-1},

† SuperCosmos Sky Survey at www-wfau.roe.ac.uk/sss, maintained by the Institute for Astronomy, Royal Observatory, Edinburgh.

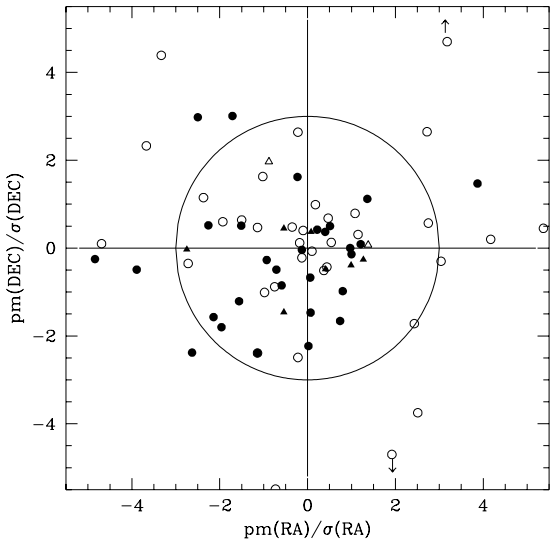

Figure 1. Proper motions for the 74 featureless continuum objects in the sample; filled triangles/circles represent objects with/without detectable radio flux and for which $\sigma < 15$ mas yr^{-1} in each co-ordinate, while open circles/open triangles are sources with $\sigma >$15 mas/yr. The circle represents the 3σ cutoff. Objects outside the circle have been removed from the sample.

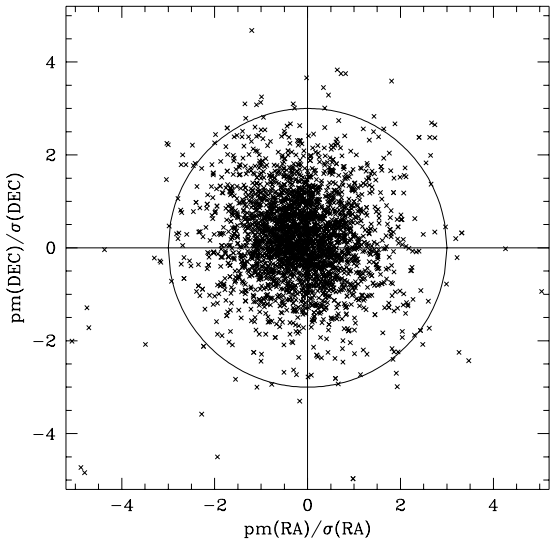

Figure 2. Proper motions for all 2QZ QSOs with $18.25 < b_J < 19.75$ and SNR ≥ 10. About 2 per cent of sources lie outside the 3σ circle and can be attributed to plate inaccuracies.

largely consistent with that expected for DC white dwarfs. One object out of the 18 exhibited a proper motion of 320 ± 80 mas yr^{-1}, but this was based on a plate pair with only a one year separation in epoch. The distribution of proper motions for our sample is shown in Fig. 1, where we plot the ratio of the proper motion to the error in each coordinate. A circle of radius 3σ then defines our proper motion cut. We test whether the distribution is consistent with the apparent proper motion distribution for all the QSOs in the

Table 1. Objects in the 2BL sample.

object	RA (2000)	dec (2000)	b_J	$u-b_J$	b_J-r	$S_{1.4}$ mJy	$S_{8.4}$ mJy	$f_x \times 10^{-12}$ ergs^{-1}cm^{-2}	z	Notes
J002522.8−284034	00 25 22.80	−28 40 34.9	18.95	−1.33	−0.12	<2.8				
J002746.6−293308	00 27 46.66	−29 33 08.4	19.08	−1.09	−0.03	<3.0				
J002751.5−293506	00 27 51.56	−29 35 06.9	18.83	−0.84	0.16	<2.8	<0.2			f
J003058.2−275629	00 30 58.27	−27 56 29.8	19.03	−0.73	0.27	<2.8	<0.2		1.577	
J004106.8−291114	00 41 06.83	−29 11 14.7	18.97	−0.71	< −2.08	<2.8	<0.2			
J004950.6−284907	00 49 50.69	−28 49 07.9	19.70	−0.53	0.52	<2.8				
J014310.1−320056	01 43 10.10	−32 00 56.7	19.36	−0.90	1.65	76.0		0.42		a
J023405.5−301519	02 34 05.58	−30 15 19.5	18.54	−0.95	0.57	<2.8			1.710	
J023536.7−293843	02 35 36.70	−29 38 43.6	18.64	−0.25	−0.63	5.0		1.0		b
J024659.5−294822	02 46 59.58	−29 48 22.6	19.90	−0.08	0.04	<3.0				
J030416.3−283217	03 04 16.33	−28 32 17.9	19.54	−0.69	0.52	8.0		2.2		c,f
J031056.9−305901	03 10 56.91	−30 59 01.3	18.70	−0.67	0.37	<3.0			>0.70	
J100253.2−001728	10 02 53.27	−00 17 28.6	19.20	−0.91	0.17	<1.0	<0.2			e
J102615.3−000630	10 26 15.34	−00 06 30.6	19.40	−0.98	0.23	<1.0				e
J103607.4+015658	10 36 07.48	+01 56 58.4	19.23	−0.94	0.66	<1.0				
J104519.7+002615	10 45 19.71	+00 26 15.0	18.68	−1.03	0.25	<1.0				e,f
J105355.1−005538	10 53 55.18	−00 55 38.5	19.53	−0.77	0.44	<1.0				f
J105534.3−012617	10 55 34.36	−01 26 17.3	18.96	−1.22	0.46	11.0		0.33		d,e,f
J110644.5+000717	11 06 44.52	+00 07 17.4	19.86	−1.11	< −1.08	<1.0				
J113413.4+001041	11 34 13.47	+00 10 41.3	18.80	−0.74	0.55	<1.0				
J113900.5−020140	11 39 00.54	−02 01 40.9	19.68	−0.48	0.92	<1.0			>0.61	
J114010.5−002936	11 40 10.51	−00 29 36.4	19.90	−1.02	−0.07	<1.0				
J114137.1−002730	11 41 37.10	−00 27 30.8	19.97	−1.55	1.26	<1.0				
J114221.4−014812	11 42 21.42	−01 48 12.2	19.30	−1.28	0.89	<1.0			1.276	
J114327.3−005050	11 43 27.30	−00 50 50.6	19.97	−0.39	0.36	<1.0			1.591	
J114521.6−024758	11 45 21.61	−02 47 58.3	18.79	−0.95	0.26	<1.0	<0.2			
J114554.8+001023	11 45 54.85	+00 10 23.6	19.59	−0.83	0.13	<1.0				
J115909.6−024534	11 59 09.61	−02 45 34.9	19.24	−0.81	0.47	<1.0				
J120015.3+000552	12 00 15.35	+00 05 52.6	19.81	−0.51	1.18	<1.0			>0.94	
J120558.1−004216	12 05 58.17	−00 42 16.3	19.11	−0.47	0.65	<1.0				f
J120801.8−004219	12 08 01.85	−00 42 19.5	18.96	−1.01	0.10	<1.0	< 0.2			f
J121834.8−011955	12 18 34.88	−001 19 55.9	19.70	−1.02	1.45	244.0				e
J122338.0−015619	12 23 38.05	−01 56 19.1	19.22	−1.16	0.37	<1.0				
J123437.6−012953	12 34 37.64	−01 29 53.1	19.44	−0.64	0.47	<1.0			>1.06	
J125435.7−011822	12 54 35.76	−01 18 22.5	19.44	−0.63	0.63	<1.0				
J130009.8−022601	13 00 09.89	−02 26 01.4	19.22	−0.66	0.55	<1.0				
J131635.1−002810	13 16 35.14	−00 28 10.6	19.82	−0.36	0.29	<1.0				f
J132811.5+000227	13 28 11.54	+00 02 27.8	19.79	−0.59	0.00	<1.0				
J140021.0+001955	14 00 21.06	+00 19 55.9	19.89	−0.97	0.59	<1.0				
J140207.7−013033	14 02 07.70	−01 30 33.3	19.71	−0.71	−0.43	<1.0				f
J140916.3−000012	14 09 16.36	−00 00 12.0	18.84	−0.60	0.37	<1.0				f
J141040.2−023020	14 10 40.28	−02 30 20.7	19.43	−1.03	0.16	<1.0	<0.2			f
J142526.2−011826	14 25 26.20	−01 18 26.3	19.91	−0.26	0.44	10.0			0.041	
J215454.3−305654	21 54 54.35	−30 56 54.3	19.55	−0.78	0.66	<2.8	<0.2			
J220515.8−311537	22 05 15.84	−31 15 37.5	19.58	−0.60	0.30	<2.5				f
J220850.0−302817	22 08 50.02	−30 28 17.6	18.40	−0.77	0.37	<2.8				
J221105.2−284933	22 11 05.25	−28 49 33.0	18.57	−0.70	0.48	81.0		0.26	>1.85	g
J221450.1−293225	22 14 50.11	−29 32 25.2	19.21	−0.37	0.79	<3.0				
J223233.5−272859	22 32 33.57	−27 28 59.9	19.33	−1.00	−0.10	<3.0				
J224559.1−312223	22 45 59.10	−31 22 23.3	19.38	−0.49	0.66	<3.0				f
J225453.2−272509	22 54 53.20	−27 25 09.4	18.83	−1.31	2.01	52.6			0.333	e
J230306.0−312737	23 03 06.04	−31 27 37.4	18.76	−0.60	0.51	<2.8			2.44?	
J230443.6−311107	23 04 43.60	−31 11 07.5	19.49	−0.85	−0.07	<2.8				
J231749.0−285350	23 17 49.00	−28 53 50.2	19.51	−0.70	−0.21	<2.8				f
J232531.3−313136	23 25 31.36	−31 31 36.0	19.54	−0.87	0.24	<3.0				
J234414.7−312304	23 44 14.70	−31 23 04.3	19.65	−0.63	0.30	5.4				

a 1RXS J014309.8−320053
b 1RXS J023536.7−293845, classification: BL Lac
c 1RXS J030416.4−283215; this object has an apparent proper motion of 2.75σ (see section 3.2) but is classified as a BL Lac
d 1RXS J105534.3−012604, classification: BL Lac
e objects with follow-up high resolution, high SNR spectra
f objects with apparent proper motion between $2-3\sigma$ (see section 2.4)
g 1RXS J221104.5-284941

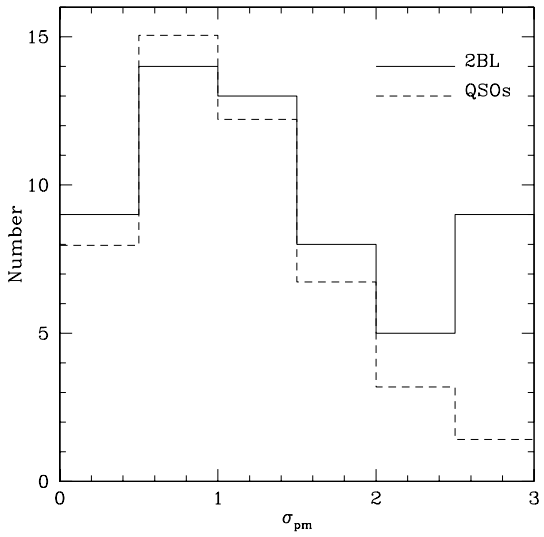

Figure 3. Histogram of proper motions for 2BL sample and 2QZ QSOs (re-normalised).

2QZ with $18.25 < b_J < 19.75$ and SNR ≥ 10, shown in Fig. 2. A 1-dimensional Kolmogorov Smirnov (KS) test on the radial distribution of proper motions in Figs. 1 and 2 revealed no significant difference at the 95 per cent confidence level between the two distributions when objects exhibiting $> 3\sigma$ proper motions are removed from both samples. For the QSOs, plate measurement errors have resulted in ~ 2 per cent of sources being attributed with $> 3\sigma$ proper motion; this is higher than would be expected for a purely Gaussian distribution.

Rejecting the 18 objects with proper motions from our data set we define a sample of 56 continuum objects with non-significant proper motions. These objects are listed in Table 1, while we list the sources with proper motions in Table 2. The sample of 56 objects we refer to below as the 2dF BL Lac (2BL) sample.

However some residual contamination of the 2BL sample is likely to remain. This is confirmed by a comparison of the QSO proper motion histogram with that of the 2BL sample (see Fig. 3). We normalised the QSO histogram to contain the same number of objects as the 2BL sample with $< 1\sigma$ proper motions. There is clearly an excess in the numbers of objects in the 2BL with $2-3\sigma$ proper motions. This excess amounts to approximately 10/56 objects or $\sim 15-20$ per cent of the sample. However, we chose not to enforce a more stringent proper motion limit on the 2BL, given the observed plate measurement errors and since two previously catalogued BL Lacs (J030416.4–283215 and J105534.3-012604) independently 're-discovered' in the 2BL, exhibit $> 2\sigma$ proper motion (33 ± 12 and $71 \pm 35\,\mathrm{mas\,yr^{-1}}$ respectively). Removing the nine radio-quiet objects with $> 2.5\sigma$, or the 12 with $> 2.0\sigma$ did not change the slope of the $n(b_J)$ relation computed for the sample (see section 4.2).

We also found that 35 per cent of the DA white dwarfs from the 2QZ in the same magnitude range as the 2BL exhibited $> 3\sigma$ proper motion. However, we cannot use this number to compute the likely number of DC white dwarfs which remain undetected in the 2BL due to low proper motions. The DA white dwarfs in the 2QZ will have absolute magnitudes up to $M_B \sim 10$ (Boyle 1989), two magnitudes brighter than the brightest DC white dwarfs. Their tangential velocity distribution is also biased towards lower velocities ($\sim 40-50\,\mathrm{km\,s^{-1}}$) than non-DA white dwarfs (Sion et al. 1988). Thus we would expect DA white dwarfs to exhibit proper motions typically up to three times less than the DC white dwarfs; $15\,\mathrm{mas\,yr^{-1}}$ for the brightest $M_B = 10$ objects and below the level of detectability with the plate material available to the 2BL. For DA white dwarfs with $M_B = 12$, the median magnitude for DA white dwarfs in the Durham/AAT survey (Boyle 1989), we would predict a mean proper motion of $\sim 40\,\mathrm{mas\,yr^{-1}}$. Thus the observation that 35 per cent of DA white dwarfs in the 2QZ have proper motions at the $30\,\mathrm{mas\,yr^{-1}}$ level or higher is consistent with a population with a median $M_B = 12$ and tangential velocity $50 \pm 10\,\mathrm{km\,s^{-1}}$.

By the same token, we anticipate that the vast majority of the DC white dwarf population with a brightest absolute magnitude of $M_B = 12$ and somewhat higher observed mean tangential velocity ($\sim 60\mathrm{km\,s^{-1}}$) will have observed proper motions at greater than the $30\,\mathrm{mas\,yr^{-1}}$ level.

We can also obtain an estimate of the catalogue completeness based on the fraction of previously known BL Lacs in the 2QZ region re-discovered by this survey. The Veron & Veron-Cetty (2001) catalogue lists 20 objects with a BL Lac or possible BL Lac identification in the region covered by the 2BL survey. Seven of these objects were classified as non-stellar in the initial measurement process of the photographic material by the APM and so were not included in the stellar catalogue from which the 2QZ was created. Only two of these non-stellar objects have magnitudes which fall within the magnitude range of the 2QZ.

As an aside we note that the 2dF Galaxy Redshift Survey independently re-discovered the six non-stellar BL Lacs that lie within the magnitude limits of that survey (Lewis I.J., private communication).

Of the remaining 13 objects classified as stellar, 11 have $u - b_J/b_J - r$ colours which place them in the locus used to define the 2QZ (see Section 4.1, Fig. 9). The two objects with colours outside this locus are both classified as BL? in the Veron & Veron-Cetty catalogue. Seven of the 11 colour-selected objects lie within the b_J magnitude limits of the 2QZ and 4 within the magnitude limits and SNR limits of the 2BL. Three of these objects (1RXS J10555−0126, 1RXS J023536.7−293845, and 1RXS J030416.4−283215) were independently re-discovered in the 2BL. The fourth (UM566), identified as a '?' in the Veron & Veron-Cetty BL Lac catalogue, was identified spectroscopically as an unambiguous DA white dwarf in the 2QZ.

If we restrict our attention to those objects with a definitive BL Lac classification in the Veron & Veron-Cetty catalogue, we find that the 2QZ colour criteria would have selected 7/7 known bona fide BL Lacs with stellar images, or 7/9 BL Lacs if we include the non-stellar BL Lacs. Extending this to include the uncertain BL Lacs as well (but excluding the known white dwarf) gives a figure of 10/12 lying within the colour critera of the 2QZ.

We therefore conclude that any incompleteness resulting from the 2QZ colour selection is low (10-15 per cent), and indeed minimal for previously confirmed BL Lacs. Furthermore all known BL Lacs which made it through the colour

Table 2. Featureless continuum objects with proper motions greater than 3σ

object	RA (2000)	dec (2000)	b_J	$u-b_J$	b_J-r	Proper motion RA arcsec yr^{-1}	Proper motion Dec. arcsec yr^{-1}
J002529.8−310433	00 25 29.85	−31 04 33.9	19.45	−0.51	0.49	0.030 ±0.012	−0.039 ±0.011
J025425.9−315834	02 54 25.99	−31 58 34.1	19.38	−1.01	0.08	0.035 ±0.013	0.031 ±0.012
J030459.3−274726	03 04 59.38	−27 47 26.2	18.86	−0.46	0.52	0.042 ±0.010	0.002 ±0.010
J031435.1−310544	03 14 35.17	−31 05 44.9	18.26	−0.82	0.02	0.030 ±0.010	−0.003 ±0.010
J102702.2+003403	10 27 02.25	+00 34 03.1	19.52	−0.89	0.34	0.323 ±0.083	0.123 ±0.083
J105037.7−011557	10 50 37.73	−01 15 57.3	19.44	−0.89	0.20	−0.088 ±0.018	−0.004 ±0.018
J113039.1−004023	11 30 39.10	−00 40 23.8	19.01	−0.71	−0.08	−0.025 ±0.015	0.043 ±0.014
J122724.0−004317	12 27 24.05	−00 43 17.4	18.68	−0.70	0.34	−0.095 ±0.024	−0.013 ±0.026
J122809.4−005407	12 28 09.44	−00 54 07.3	19.21	−1.48	−0.01	−0.076 ±0.029	−0.073 ±0.031
J124034.9−014500	12 40 34.96	−01 45 00.9	19.47	−0.76	0.18	−0.061 ±0.013	0.001 ±0.012
J132023.7+001606	13 20 23.70	+00 16 06.4	19.33	−0.97	0.29	−0.035 ±0.010	0.042 ±0.010
J132326.9−004157	13 23 26.96	−00 41 57.7	19.44	−0.82	0.20	−0.008 ±0.011	−0.054 ±0.010
J132849.0−002427	13 28 49.05	−00 24 27.2	19.56	−0.71	0.51	0.022 ±0.011	−0.069 ±0.010
J133703.1−003910	13 37 03.16	−00 39 10.8	19.08	−0.94	0.01	−0.040 ±0.016	0.044 ±0.015
J142127.9−020033	14 21 27.99	−02 00 33.9	18.85	−1.00	−0.01	−0.036 ±0.010	0.020 ±0.009
J215530.4−312148	21 55 30.49	−31 21 48.6	18.70	−0.33	0.01	0.054 ±0.010	0.004 ±0.009
J231219.3−280928	23 12 19.36	−28 09 28.1	19.08	−0.71	0.34	−0.027 ±0.011	−0.045 ±0.010
J233139.6−272018	23 31 39.63	−27 20 18.3	18.83	−0.77	0.19	0.035 ±0.011	0.087 ±0.010

selection process, and fulfilled the magnitude and SNR criteria of the 2BL, were classified as BL Lacs.

2.5 Cross-correlation with radio and X-ray surveys

For each object in the 2BL sample a search was performed using the NVSS[‡] and (where applicable) FIRST[§] databases. Initially nine matches were found in NVSS with no additional matches in FIRST, and all were within a radius of 11 arcsec (search conducted out to 15 arcsec). Subsequent inspection of all NVSS and FIRST radio maps at the coordinates of our sources revealed no detections above the rms noise levels, nevertheless a conservative 5σ detection limit was adopted for the 46 non radio-detected 2BL objects, as listed in Table 1. A further cross-correlation of 2BL sources was carried out with the *ROSAT* bright and faint all sky X-ray catalogues (Voges et al. 1999), initially using a 40 arcsec radius. All five matches found were, however, within a 15 arcsec radius. A search out to 60 arcsec revealed no further matches. All five objects with a detectable X-ray flux are radio sources, consistent with the observation that all X-ray selected BL Lacs are radio-loud (Stocke et al. 1990). Two of these objects with both radio and X-ray flux are listed in the literature as BL Lacs (see Table 1).

3 RADIO AND OPTICAL OBSERVATIONS

3.1 2dF observations

The 2dF spectra for the 56 objects in the 2BL sample are plotted in Appendix A. A number of objects (12/56) also have a second (or third) observations with 2dF with SNR of least 5. These are also shown in Appendix A. Of the four objects which have two or more SNR > 10 spectra, three (J002751.5–293506, J100253.2–001725 and J114137.1–002730) had both spectra (in one case all three) independently identified as belonging to a continuum source. In the fourth case (J023405.5-301519) one spectrum displays broad lines of C III] and C IV at $z = 1.710$ (see below). Of the eight objects with additional lower SNR spectra (5 <SNR< 10), two (J003058.2–275629 and J114327.3–005050) show evidence for broad emission lines. We have further examined all the available 2dF spectra to identify weak lines indicating a redshift, or absorption lines from intervening systems placing a lower limit on a redshift. As well as intrinsic redshift measurements we should also expect that if the 2BL sample is largely composed of extragalactic sources a number should also show narrow metal absorption systems, e.g. Mg II or C IV, or indeed Lyman α for objects with $z > 2.1$. These can then be used to place a lower limit on an object's redshift. In their analysis of the QSOs in the 2QZ 10k catalogue, Outram et al. (2001) find that 11 per cent of QSOs at $z > 0.5$ with SNR > 15 have significant narrow absorption line systems with more than one absorption line. This then suggests that we should find $\sim 4-5$ sources in the 2BL with these features.

Below we discuss the individual sources which show emission or absorption features:

J003058.2–275629 has two 2dF spectra, of which one shows clear evidence of broad C III] and C IV emission lines at $z = 1.577$. With knowledge of its redshift, it is possible to see weak C III] ($W_\lambda \sim 4$Å [rest frame]) and (tentatively) weak C IV in the higher SNR spectrum, from which the original continuum ID was made. There thus appears to be continuum variability in this source.

J023405.5-301519, as noted above, shows broad C III] and C IV emission at $z = 1.710$ in one spectrum. There is no evidence of these features in the other 2QZ spectrum of

‡ NRAO/VLA Sky Survey (Condon et al. 1998)
§ Faint Images of the Radio Sky at 20cm (White et al. 1997)

this object. We class this a source with variable continuum emission.

J031056.9–305901 has a number of narrow absorption lines, most probably due to intervening absorbers. The absorber at 4760Å could be either Mg II or C IV, suggesting a lower limit on the redshift of $z > 0.70$.

J113900.5–020140 has one strong absorption line visible at 4500Å in both spectra. A redshift lower limit of $z > 0.61$ may be set assuming this feature is due to the Mg II doublet.

J114221.4–014812 exhibits a single very weak emission line ($EW_{\rm rest} = 4$Å) at 6370Å. Assigning this to Mg II we derive a redshift of $z = 1.276$. However, we see no corresponding C III] emission at this redshift.

J114327.3–005050 has two spectra, of which one shows broad C III] and C IV emission at $z = 1.591$. The other spectrum shows no evidence of emission lines. This object is therefore classed as variable.

J120015.3+000552 shows an absorption doublet at 5400Å which corresponds to Mg II at $z = 0.94$. There is also a weak Fe II 2600Å absorption line at the same redshift. The redshift of this object is thus $z > 0.94$.

J123437.6–012953 contains a system with Mg II, Fe II 2600Å and Fe II 2383Å absorption at $z = 1.06$, which defines a lower limit to the redshift of this object.

J142526.2–011826 shows narrow Hα and [O II] yielding a low redshift of $z = 0.041$. In this case the Ca II H&K break contrast is negligible, consistent with the operational definition for BL Lac classification (Morris et al. 1991).

J221105.2–284933 contains a strong absorption system at $z = 1.85$ with C IV, Al II 1671Å and Fe II 2344, 2383, 2587 and 2600Å. On the blue wing of the C IV absorption line is an emission feature which could be intrinsic C IV emission, however, no other emission features are found, and the rest equivalent width of the line is only 1.6Å. We therefore use $z = 1.85$ as a lower limit to the redshift of this object, noting however that this absorption may be intrinsic to the source.

J230306.0–312737 shows features bluewards of 4250Å which could be Lyα absorption. There is also a bump at 5320Å which could be associated with C IV at $z = 2.44$, however this would imply that any Lyα emission has been absorbed. Although this object may be identified as a QSO at $z = 2.44$, we choose to leave it in the current sample given the uncertainty of its identification. Removal of this object from the 2BL has no effect on our conclusions.

For the objects which appear to vary we have confirmed that the featureless nature of the spectra is not an artifact of the data-reduction process, so that the difference between the two spectra appears to be real. We interpret this as due to continuum variablity, with the broad emission lines appearing when the continuum is in its low state - behaviour also shown by the prototype of the BL Lac class (Corbett et al. 2000). Indeed it is possible that the variable nature of the continuum in these sources has caused us to miss potential members of this class when classification is made from a single spectrum. Continuum variability would tend to give rise to an enhanced visibility of emission lines in spectra taken in a low continuum state – corresponding to a lower SNR spectrum for a survey with largely fixed exposure times.

Of the 12 2BL objects for which we have two or more spectra (26 spectra in total), three show some evidence for continuum variability which would have resulted in a QSO, rather than a continuum classification. Given that this behaviour is observed in the prototype of the class, we choose to retain these objects in the 2BL. Although based on a small sample (3 spectra out of 26), we estimate that continuum variability may lead to a potential 10–15 per cent incompleteness due to mis-classification in the 2BL.

The number of 2BL sources which contain metal absorption lines is broadly consistent with that expected and we note that a similar radio-quiet continuum source has been found by Croom et al. (in preparation) in the 2QZ. This object falls below the magnitude limit of the 2BL, but shows a red continuum with C IV and Al III absorption at $z = 1.89$, confirming that such high redshift continuum sources do exist. We further note that Fan et al. (1999) have found a "quasar without emission lines" at $z = 4.62$ in data from the Sloan Digital Sky Survey.

3.2 Higher signal-to-noise spectroscopy

Despite the anticipated difficulty of obtaining redshifts for the 2BL sample, we nevertheless began a campaign to obtain higher signal-to-noise, higher resolution spectra of as many of the 2BL sample as possible. We can use these observations to place yet more stringent limits on the featureless nature of the optical spectra and obtain an independant measure of the likely contamination level of the 2BL by galactic stars.

One candidate BL Lac (J225453.2–272509) was observed in August 2000 using the long slit, double-beam spectrograph (DBS) on the Mt Stromlo 2.3m telescope at Siding Spring. The object was observed for a total of two hours with resolutions of 4.1 and 4.5 Å pixel^{-1} in the blue (3800–6100Å) and the red (6200–8500Å) arms of the DBS respectively. Data reduction was performed using standard IRAF¶ procedures (*ccdred* and *apall*).

J225453.2–272509 was confirmed as having no emission lines and we were able to measure a redshift of $z = 0.333$ from Ca II H & K and G band absorption features.

A further 4 BL Lac candidates were observed on 2001 February 21–22 using the ISIS double-beam spectrograph on the William Herschel Telescope. These spectra covered the range 3800Å–5000Å and 6300Å–8000Å in the blue and red arms respectively at a spectral resolution of 1Å pixel^{-1}. Exposure times of 20 minutes were sufficient to yield a SNR >25 in the continuum of these objects.

Two candidates in the 2BL sample (J105534.3–012617 and J121834.8–011955) had also been observed with Keck as part of a follow-up of radio-loud 2QZ sources (Brotherton et al. 1998). The first of these two was one of the sources also observed with the WHT.

These 7 objects represent 12.5 per cent of the 2BL sample. Apart from the Keck spectra, the objects on which follow-up spectroscopy was obtained were selected at random from the 2BL. Of the five objects selected at random,

¶ IRAF is distributed by the National Optical Astronomy Observatories,operated by the Association of Universities for Research in Astronomy Inc., under cooperative agreemfent with the National Science Foundation

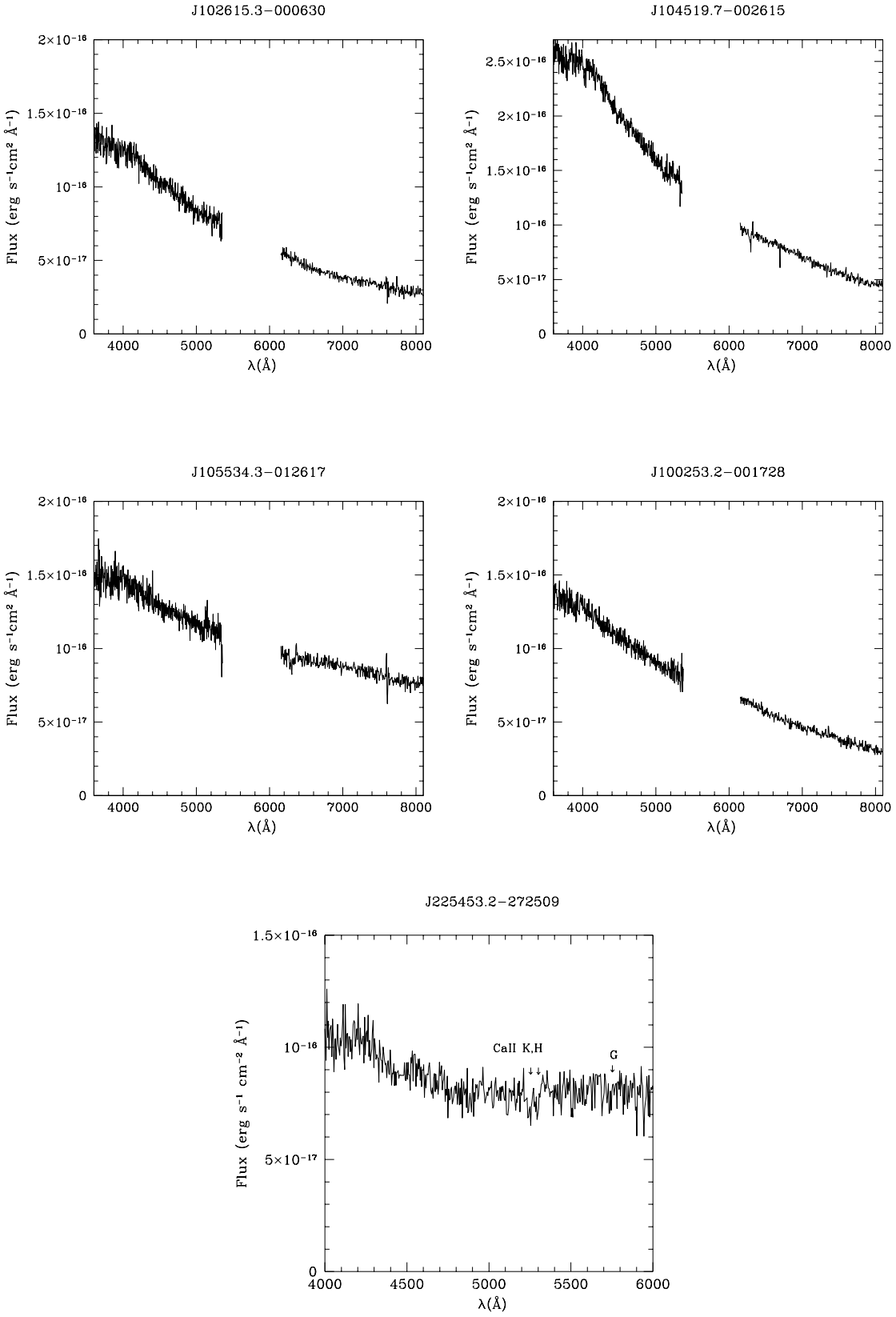

Figure 4. Follow up high-resolution, high signal-to-noise spectra for five sources in our sample (four WHT and one MSSSO 2.3m spectra).

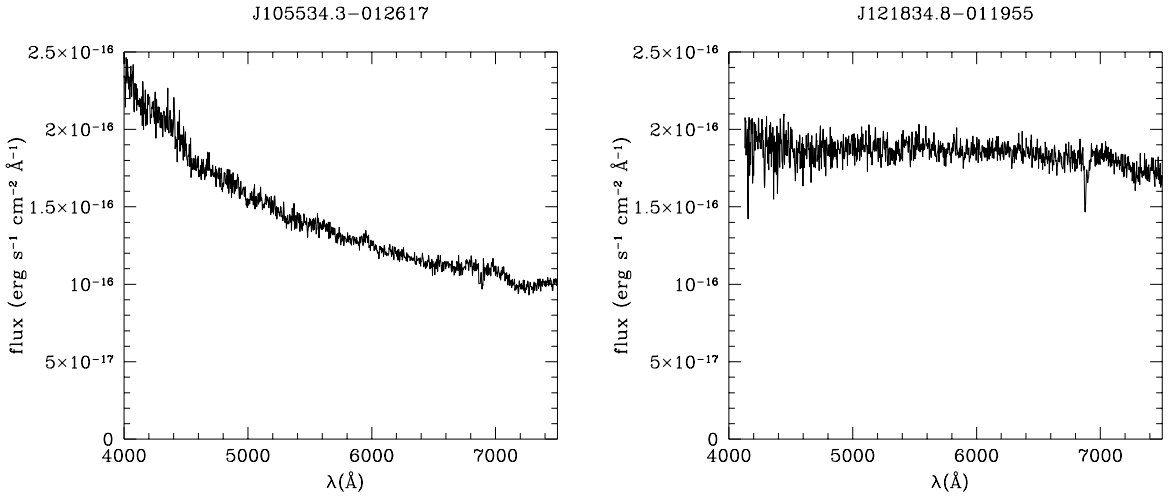

Figure 5. The two radio loud objects observed with Keck by Brotherton et al. 1998. The feature at $\sim$ 6900Å is a telluric absorption band.

all exhibit spectra consistent with a continuum source identification.

We are thus able to obtain possible redshifts/limits for 12 objects in this sample, covering a relatively wide range in redshift; from $z = 0.041$ to $z > 2.4$, with a median $z = 1.2$ (assuming that objects with lower limits are at that limiting redshift). Of these, only two are detected radio sources (J225453.2–272509, $z = 0.333$ and J221105.2–284933 at $z > 1.85$).

From the optical spectroscopic observations and the proper motion study above we can place a limit on the likely contamimation of the sample by weak-lined Galactic subdwarfs and white dwarfs of 10 – 20 per cent. Although both are subject to large uncertainties, we note that this limit on the contamination level is similar to the potential incompleteness level caused by continuum variability (see above). In the statistical analysis below, we therefore choose not to correct the numbers in the 2BL for either incompleteness or contamination. However we do note that the numbers/normalisation of the 2BL sample carry an uncertainty at least at the $\pm$20 per cent level.

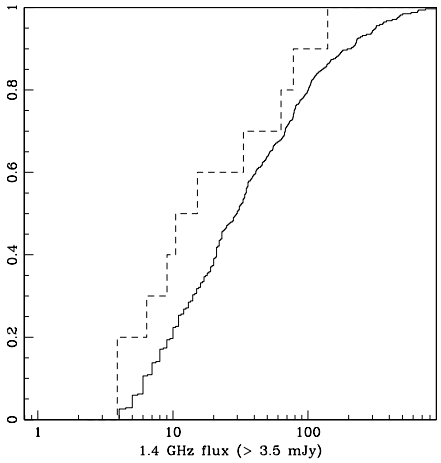

Figure 6. Cumulative distribution of the 340 radio loud QSOs and the 9 BL Lac candidates (dashed line) with $S_{1.4GHz} >$ 3.5mJy

3.3 Radio observations at 8.4 GHz

Observations of a sub-sample of eight 2BL objects were made at a frequency of 8.4 GHz using the NRAO Very Large Array on 2001 January 28. The array was in a hybrid BnA→B configuration with 25 antennas operating. BL Lac candidates from the equatorial strip were observed for 32 minutes each while those from the southern strip ($-27^o < \delta < -31.5$) were observed for 40 minutes, in both cases in snapshot mode. Flux densities were bootstrapped from 3C286. The typical noise level in each snapshot was 45μJy. Data were reduced using the ATNF's[‖] MIRIAD software package (Sault, Teuben & Wright 1995), following standard procedues from the Miriad User's Manual (Sault and Killeen 1999).

We found no detections at the positions of the candidate BL Lac sources with a flux density $> 5\sigma$ ($\simeq$ 0.2mJy) above the background noise level. Results are included in Table 1.

A comparison of the radio flux distributions of the nine radio-loud objects in the 2BL and the 340 radio-loud QSOs with $b_J < 20.00$ and $S_{1.4} > 3.5$mJy in the 2QZ is shown in Figs. 6 and 7. A KS test revealed no significant difference between the two populations.

For the one object in the 2BL sample with a measured redshift and documented NVSS flux density of 52.6mJy, we obtain a radio power $P_{1.4} = 2.5 \times 10^{25}$ W Hz^{-1}, and $M_B = -22.05$ (using $\Omega_m = 1$, $\Omega_\Lambda = 0$, $H_0 = 50\,\mathrm{km\,s^{-1}Mpc^{-1}}$,

[‖] Australia Telescope National Facility

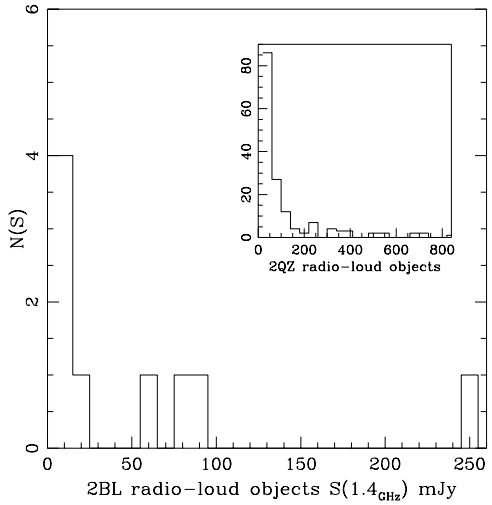

Figure 7. Differential distribution of the 340 radio loud QSOs and the 9 BL Lac candidates

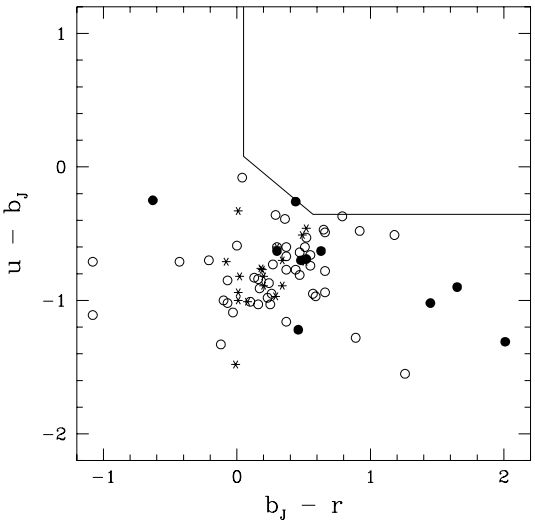

Figure 8. $u - b_J$, $b_J - r$ plot of BL Lac candidates; filled circles represent 2BL objects with radio detections (1.4 GHz) while open circles represent radio-quiet objects. Asterisks are the 18 featureless continuum objects with proper motion which have been removed from the 2BL sample. The straight lines are the 2QZ colour selection cut-off.

$\alpha_r = -0.5$, $\alpha_{opt} = -0.5$). This value lies at the upper end of the range of 1.4 GHz radio powers calculated for the EMSS BL Lacs (Rector et al. 2000) which range from 4 $\times 10^{23}$ W Hz^{-1} to 3 $\times 10^{25}$ W Hz^{-1} using the same cosmology.

4 BASIC PROPERTIES OF THE 2BL

4.1 Colour distribution

In Fig. 8 we show the u-b_J[⋆⋆], b_J-r colour distribution of 2BL sources. Open circles represent candidate BL Lacs with no radio detection, while filled circles denote those objects with a measured radio flux density ($S_{1.4} > 1.5$mJy); asterisks represent the 18 objects which were found to have significant proper motion and subsequently removed from the sample. A 2-D KS test on the $u - b_J/b_J - r$ distributions of these 18 objects and the 56 objects in the 2BL sample returned a 95 per cent probability that the two distributions are different; this increased to 97 per cent if only those 2BL objects with $< 2\sigma$ proper motions were considered.

As a comparison, the $u - b_J/b_J - r$ distribution of the 13 BL/BL? objects from the Veron & Veron-Cetty catalogue discussed in section 2.4 is plotted in Fig. 9.

Three of the four strong radio sources ($S_{1.4GHz} > 50$ mJy) show evidence of an enhanced red component while still exhibiting a strong UV flux. A comparison with the colours of Galactic sub dwarfs (Fig. 10) shows that the 2BL is unlikely to be heavily contaminated by this population. Less than 10 per cent of the 2BL sample exhibit colours in the densely populated locus of the Galactic subdwarfs. The region populated by the DA white dwarfs identified in the 2QZ (see Croom et al. 2001) is also shown (Fig. 11). For a given $u-b_J$, the mean b_J-r colour for 2BL objects is approximately 0.4 mag redder than that of the DA white dwarfs. A 2-D KS test on colour distributions of the 2BL objects and

⋆⋆ u=U-0.24 (Smith et al. 2001)

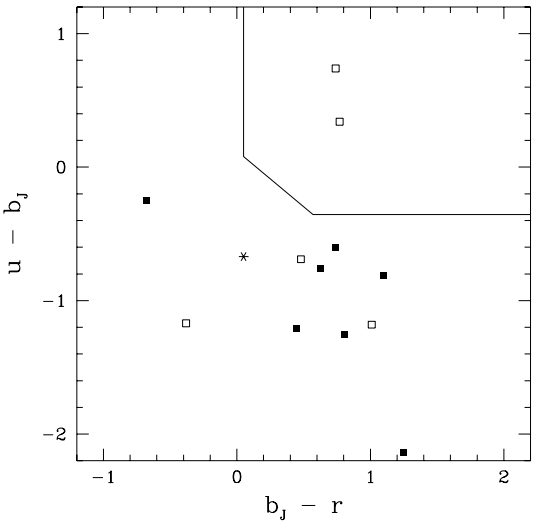

Figure 9. $u - b_J$, $b_J - r$ plot of the 13 objects from the Veron & Veron-Cetty (2001) catalogue included in the 2QZ input catalogue. Solid squares represent a BL classification while open squares refer to BL? objects. The mis-identified white dwarf is shown as an asterisk.

the 2QZ DA white dwarfs returned a > 99.9 per cent probability that the two distributions are different. A similar 2-D KS test was carried out on the 56 2BL objects and the 10 BL/BL? objects from the Veron & Veron-Cetty catalogue that satisfy the 2QZ colour selection criteria (Fig. 9), but excluding the white dwarf. The test revealed no significant difference betwen the two distributions.

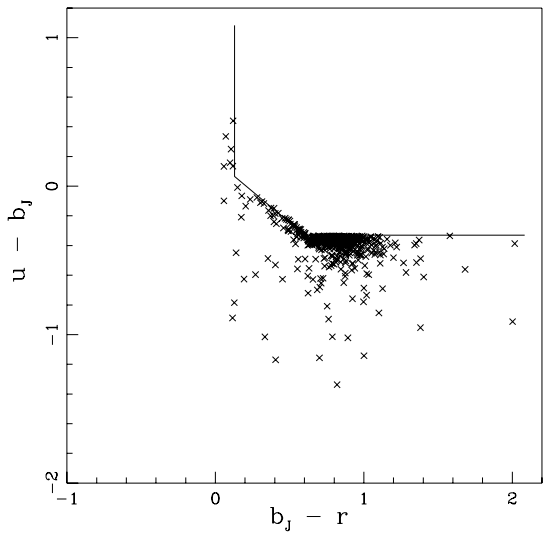

Figure 10. $u - b_{\rm J}$, $b_{\rm J} - r$ diagram of F and G type stars in the 2QZ with SNR > 10.

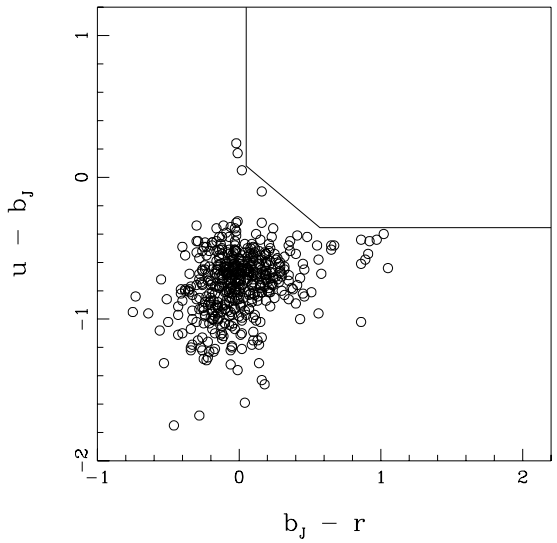

Figure 11. $u - b_{\rm J}$, $b_{\rm J} - r$ diagram of DA white dwarfs in the 2QZ with SNR > 10.

4.2 Optical $n(b_{\rm J})$ relation

The differential number magnitude, $n(b_{\rm J})$, relation for the 2BL is plotted in Figure 12. The $n(b_{\rm J})$ relation is normalised to the fractional number of objects with signal-to-noise ratio greater than 10 in each 0.25 mag bin:

$$n(b_{\rm J}) = \frac{N_{\rm obs}(b_{\rm J})}{544\ {\rm deg}^2} \times \frac{N_{\rm TOT}(b_{\rm J})}{N_{\rm SNR\geq 10}(b_{\rm J})} \qquad (1)$$

as set out in Table 3.

Based on a weighted least squares fit of the 2BL $n(b_{\rm J})$ we measured a slope of $n \propto 10^{0.66\pm0.10m}$. In order to check the robustness of the $n(b_{\rm J})$ relation against choice of signal-to-noise limit, we derived the $n(b_{\rm J})$ relation for the sample of 27 candidate 2BL objects with SNR > 15. The best fit displayed an almost identical slope and normalization, $n(b_{\rm J}) \propto 10^{0.71\pm0.24m}$, to that obtained for the SNR ≥ 10 sample. The steepness of the $n(b_{\rm J})$ relation is also robust against choice of survey magnitude limits; a least squares fit to only those points with $b_{\rm J} < 19.5$ yielded a slope of 0.64 ± 0.25. Rejecting the 12 radio-quiet 2BL objects with proper motions of $2\sigma - 3\sigma$ produced a slope of 0.68 ± 0.09, hence almost identical to that of the full sample of 56 objects.

The $n(b_{\rm J})$ relation for all DA white dwarfs with SNR$>$ 15 in the 2QZ is plotted in Fig. 12. This SNR was chosen to ensure minimal contamination of the white dwarf sample by subdwarfs which can be increasingly confused with white dwarfs in the 2QZ sample for SNR$<$ 15 (Vennes et al., in preparation). The white dwarf $n(b_{\rm J})$ relation exhibits a slope of $n \propto 10^{0.37\pm0.07m}$, significantly flatter than the $n \propto 10^{0.66\pm0.10m}$ slope of the 2BL objects. Indeed, a minimum χ^2 fit between the $n(b_{\rm J})$ relations for the 2QZ white dwarf and 2BL samples reveals that they are different at the 99 per cent confidence level.

We also plot in figure 12 the re-normalised $n(b_{\rm J})$ relation for the 2QZ QSOs based on a minimum χ^2 fit to the 2BL counts. The χ^2 test confirms that the 2BL and re-normalised 2QZ $n(b_{\rm J})$ relations are consistent with each other, with a relative normalisation of 0.014.

Table 3. Observed and computed number counts; N_{TOT} refers to the number of 2QZ objects in the respective magnitude range, and $N_{\rm SNR\geq 10}$ to those which also satisfy the criterion of SNR $\geq$10. N_{obs} is the number of featureless continuum objects (i.e. BL Lac candidates) identified from the SNR $\geq$10 spectra, and $n(b_{\rm J})$ is computed as given in equation (1). The errors are 1σ Poisson errors (Gehrels 1986).

0.25 mag bin	$N_{\rm TOT}$	$N_{\rm SNR\geq 10}$	N_{obs}	log $n(b_{\rm J})$
$18.25 < b_{\rm J} \leq 18.50$	936	819	$1\ ^{+2.30}_{-0.83}$	–2.08
$18.50 < b_{\rm J} \leq 18.75$	1091	844	$5\ ^{+3.38}_{-2.16}$	–1.32
$18.75 < b_{\rm J} \leq 19.00$	1368	988	$10\ ^{+4.27}_{-3.11}$	–0.99
$19.00 < b_{\rm J} \leq 19.25$	1759	1040	$9\ ^{+4.11}_{-2.94}$	–0.95
$19.25 < b_{\rm J} \leq 19.50$	2433	1116	$9\ ^{+4.11}_{-2.94}$	–0.84
$19.50 < b_{\rm J} \leq 19.75$	3255	1106	$12\ ^{+4.56}_{-3.41}$	–0.59
$19.75 < b_{\rm J} \leq 20.00$	4012	859	$10\ ^{+4.27}_{-3.11}$	–0.46

Sample	slope	σ
2BL	0.66	0.10
2QZ QSOs	0.59	0.03
2QZ WDs	0.37	0.07

Table 4. Comparison of $n(b_{\rm J})$ values, $n \propto 10^{slope*m}$, for the 2BL objects, the 2QZ white dwarfs and QSOs in Fig. 12.

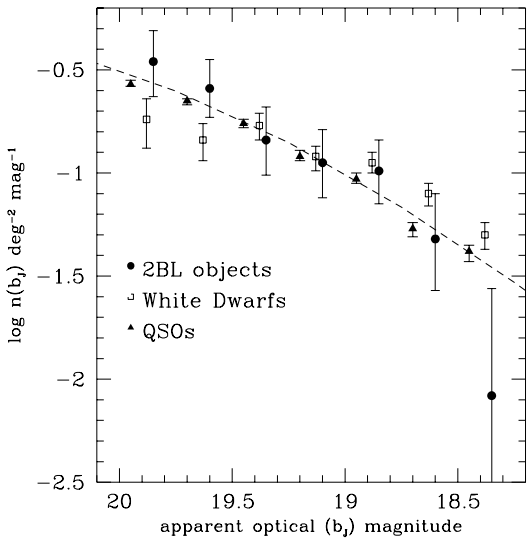

Figure 12. The $n(b_J)$ relation for 2dF QSOs normalised by 0.014 (triangles) and 2QZ white dwarfs (open squares), normalised by 0.12, plotted against the 2BL sample and the predicted $n(b_J)$ relation from Boyle et al. (2000) (dashed line). The choice of normalising factor was made in order to minimize the χ^2 statistic between the 2 distributions. For clarity 2BL objects are offset by 0.03 mag relative to the white dwarfs. The QSO number counts are from Boyle et al. (2000)

4.3 Predicted redshift distribution

Given the similarity between the $n(b_J)$ relations for the 2BL sample and 2QZ QSOs, we used the evolutionary model derived for the latter to obtain a prediction of the redshift distribution for the 2BL. In doing this we assume that the vast majority of 2BL objects represent a sample of AGN with very weak or absent emission lines and hence exhibit the same evolutionary behaviour (Croom et al. 2001) and identical form of luminosity function (LF) to that obtained for the 2QZ QSOs (see Boyle et al. 2000). To give the observed total number objects in the 2BL we used a normalisation 0.015 times (consistent with the χ^2 fitting above of 0.014) that of the QSO LF (i.e. $\Phi^*_{2BL} = 1.65 \times 10^{-8}\mathrm{mag}^{-1}\mathrm{Mpc}^{-3}$), with an identical break luminosity, $M^*_{(z=0)} = -21.9$. A χ^2 test confirmed that the predicted $n(b_J)$ relation based on this model (also plotted in Fig. 12) is consistent with the observed 2BL $n(b_J)$ relation.

The predicted number-redshift, $n(z)$, relation for the 2BL sample based on this model is shown in Fig. 13. In common with the QSOs at similar magnitudes ($b_J < 20$), the $n(z)$ relation is predicted to peak at $z = 1.6$ with a median redshift of $z = 1.1$. The decline in the $n(z)$ at higher redshifts results from a combination of factors: the depth of the sample, the slow-down in the QSO evolution rate at $z > 2$ and the k-correction in the B-passband due to the Lyman α forest. The bimodal nature of the $n(z)$ relation is an artefact of the strong magnitude dependence of the areal coverage function in the 2BL.

If the extragalactic objects in the 2BL sample are distributed with this $n(z)$ relation it will be hard to obtain redshifts/unambiguous identifications for these objects from their optical spectra alone unless they exhibit intervening

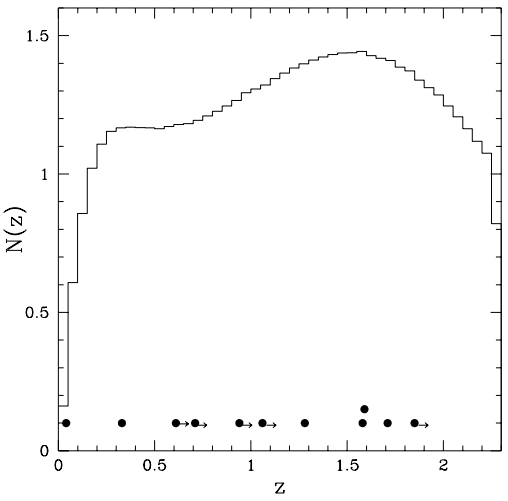

Figure 13. Predicted redshift distribution of 2dF BL Lac candidates using the evolution model of Boyle et al. (2000); dots and dots with arrows indicate the actual measured redshifts/lower limits for 2BL objects.

absorption line systems. Previously, many BL Lac redshifts have been based on spectroscopic features in the host galaxy (e.g CaII H&K, G band). The 2dF spectra on which the selection of the sample was based cover the region 3800–7800Å (with the region redward of 6800Å increasingly contaminated by night sky emission). If one requires both CaII H&K and the G band to be detected for a secure identification/redshift, then this would only be possible in the 2dF spectra for objects with $z < 0.5$, less than 10 per cent of sample predicted by the $n(z)$ relation.

Nevertheless, the small number of tentative redshifts or lower limits on redshifts obtained for objects in the 2BL to date is certainly not inconsistent with the proposed redshift distribution (see Fig.13).

5 DISCUSSION

The 2BL sample is a unique, optically selected sample of featureless continuum objects. Follow-up optical spectroscopy at higher resolution and SNR confirms the featureless nature of a subsample of these objects, while the broadband optical colours of these objects are inconsistent with Galactic subdwarfs. The steep $n(b_J)$ relation of this population implies strong cosmlogical evolution, consistent with that of QSOs and indicative of a population that is extragalactic in origin. Based on a QSO evolution model the median redshift of the sample is predicted to be $z \sim 1.1$. In all respects, other than their radio properties, the majority of the 2BL objects are consistent with the class of objects known as BL Lacs.

Hitherto there has been no large optically-selected sample of BL Lacs. Previously all BL Lacs have been initially identified by their radio or X-ray emission. Moreover, all the BL Lacs identified to date have shown strong radio emission. Indeed Stocke et al. (1990) have argued that there are no radio-quiet BL Lacs on the basis that all BL Lacs identified in the EMSS had radio flux densities of $S_{5\mathrm{GHz}} > 1\,\mathrm{mJy}$.

Notably all five 2BL objects with X-ray detections

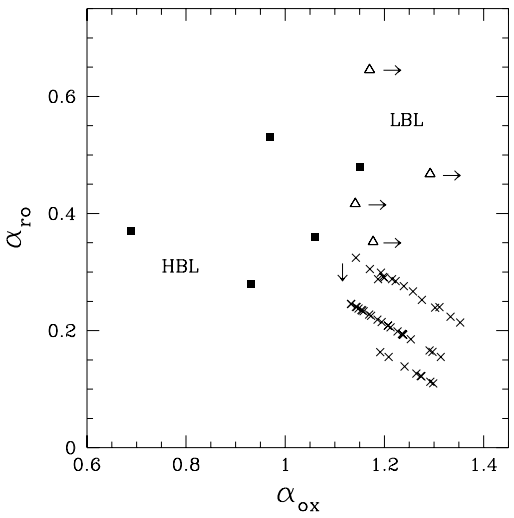

Figure 14. $\alpha_{\rm ro} - \alpha_{\rm ox}$ diagram (1.4 GHz, 4400 Å, 2Kev) of the 2BL sample. Five sources (solid squares) have both X-ray and radio flux; open triangles denote sources with a radio detection and right arrows denote upper limits of $f_x = 8 \times 10^{-14}$ erg s^{-1} cm^{-2}; in addition crosses have a limiting radio flux density as per Table 1; $S_{8.4}$ limiting fluxes of 0.2 mJy, have been converted to a 1.4GHz flux density of 0.5 mJy using $\alpha_r = -0.5$

(based on the *ROSAT* All Sky Survey, RASS) are also milli-Jansky radio sources. The flux limit of the RASS ($S_{0.1-2.4{\rm keV}} = 8 \times 10^{-14}\,{\rm erg\,s^{-1}\,cm^{-2}}$) is equivalent to $S_{0.3-3.5{\rm keV}} = 6.2 \times 10^{-14}\,{\rm erg\,s^{-1}\,cm^{-2}}$ for an object with an X-ray spectrum of $f_\nu \propto \nu^{-1}$, hence almost identical to the EMSS flux limit.

In Fig. 14 we plot the X-ray-to-optical $\alpha_{\rm ox}$ and radio-to-optical $\alpha_{\rm ro}$ flux ratio for the sample, where we have defined $\alpha_{\rm ro}$ as $[\log(S_{1.4}/f_{4400\mathring{\rm A}})]/5.7$ and $\alpha_{\rm ox}$ as $[\log(f_{4400\mathring{\rm A}}/f_{2keV})]/2.85$. In the absence of redshift information k-corrections have not been applied, however with $\alpha_{opt} = \alpha_r = -0.5$ and $\alpha_x = -1$ corrections at $z = 1.1$ amount to less than -0.05 for α_{ox}. In common with Stocke et al. (1990) we find that our bright X-ray detected BL Lacs exhibit a narrow range in radio–optical spectral index, namely $0.28 < \alpha_{\rm ro} < 0.53$.

At the predicted median redshift of the 2BL ($z = 1.1$), the 5σ 0.2 mJy detection limit of the VLA observations corresponds to an upper limit for the radio power of $P_{1.4{\rm GHz}} \leq 1.7 \times 10^{24}\,{\rm W\,Hz^{-1}}$. This is still within the range of radio powers for the EMSS BL Lac sample observed by Rector et al. (2000). Thus high redshift BL Lacs with radio powers similar to those low redshift BL Lacs found by Rector et al. (2000) could still have evaded detection at deepest radio flux limits probed by our VLA observations. However, these high redshift objects would have a lower $\alpha_{\rm ro}$ than BL Lac objects observed to date, and would constitute a distinct population, occupying a different region of the $\alpha_{\rm ro} - \alpha_{\rm ox}$ plane to that of hitherto known BL Lac objects. The continuum emission mechanism that would produce such radio-weak objects is unclear; these objects may simply be a class of lineless QSOs with an optical continuum mechanism (e.g. hot accretion disk) very different to that producing the optical radiation in objects hitherto identified as BL Lacs.

While the nature of the 2BL objects with no detectable radio emission remains uncertain, it appears that those objects with radio detections are bona fide BL Lacs, and are some of the optically faintest BL Lacs detected to date. In addition, of the 11 or 12 2BL objects that have redshift information (and hence appear to be extragalactic), 10 are at a redshift greater than 0.6, a region generally thought to be sparsely populated by BL Lac objects.

If the radio-quiet objects are not AGN, then the question remains as to their nature. If they are DC white dwarfs, or indeed any class of Galactic star, then there is perhaps an even greater puzzle in explaining the steep $n(b_{\rm J})$ relation. Further observations of the 2BL sample including infrared photometry and spectroscopy (to attempt to detect the host galaxy) and/or variability and polarisation studies may help to resolve their identity.

ACKNOWLEDGEMENTS

The 2QZ is based on observations made with the Anglo-Australian Telescope and the UK Schmidt Telescope; we would like to thank our colleagues on the 2dF galaxy redshift survey team and all the staff at the AAT who have helped to make this survey possible. We thank the anonymous referee for a careful scrutiny of the manuscript and his/her insightful comments which have greatly improved the contents and clarity of the paper. DL thanks the School of Physics at the University of Sydney for a Postgraduate (Mature Age) Scholarship.

REFERENCES

Bade N., Beckmann V., Douglas N.G., Barthel P.D., Engles D., Cordis L., Nass P. Voges W., 1998, A&A, 334, 459
Bailey J. et al., 2002, MNRAS, submitted
Becker R.H., Gregg M.D., Hook I.M., McMahon R.G., White R.L., Helfand D.J., 1997, ApJ, 479, L93
Boyle B.J., 1989, MNRAS, 240, 533
Boyle B.J., Shanks T., Croom S.M., Smith R.J., Miller L., Loaring N., Heymans C., 2000, MNRAS, 317, 1014
Brotherton M.S., van Breugel W., Smith R.J., Boyle B.J., Shanks T., Croom S.M., Miller L., Becker R.H., 1998, ApJL, 505, 7
Browne I.W.A, , Marchã M.J.M., 1993, MNRAS, 261, 795
Condon J.J., Cotton W.D., Greisen E.W., Yin Q.F., Perley R.A., Broderick J.J., 1998, AJ, 115, 1693
Corbett E.A., Robinson A., Axon D.J., Hough J.H., 2000, MNRAS, 311, 485
Croom S.M., Smith R.J., Boyle B.J., Shanks T., Loaring N.S., Miller L., Lewis I.J., 2001, MNRAS, 322, L 29
Fan X., et al., 1999, ApJ, 526, L57
Fanaroff B.L., Riley J.M., 1974 MNRAS, 167, 31
Fosatti G., 2001, in Padovani P. and Urry M., eds., ASP Conf. Ser. Vol 227 Blazar Demographics and Physics. Astron. Soc. Pac., San Francisco, p.218
Gehrels N., 1986, ApJ, 303, 336
Giommi P., Pellizzoni A., Perri M., Padovani P., 2001, in Padovani P. and Urry M., eds., ASP Conf. Ser. Vol 227 Blazar Demographics and Physics. Astron. Soc. Pac., San Francisco, p.227
Laurent-Muehleisen S.A., Kollgaard R.I., Fiegelson E.D., Brinkmann W., Sibert J., 1999, ApJ, 525, 127
Lewis I. J. et al., 2001, MNRAS, submitted (astro-ph 0202175)

Maccacaro, T., della Ceca, R., Gioia, I.M., Morris, S.L., Stocke, J.T., Wolter, A., 1991, ApJ, 37,. 117
McCook G.P., Sion E.M., 1999, ApJS, 121, 1
Marchã M.J.M., , Browne I.W.A., 1995, MNRAS, 275, 951
Miller, L., Peacock, J.A., Mead, A.R.G., 1990, MNRAS, 244, 207
Morris et al., 1991, ApJ, 380, 49
Outram P.J., Smith R.J., Shanks T., Boyle B.J., Croom S.M., Loaring N.S., Miller L., 2001, MNRAS, 328, 805
Padovani P., Giommi P., 1995 ApJ, 444, 567
Rector T.A.,Stocke J.T., Perlman E.S.,Morris S.L., Gioia I.M., 2000, AJ, 120, 1626
Rector T.A., Stocke J.T., Perlman E.S., 1999, ApJ, 516, 145
Rector T.A. , Stocke J.T., 2001, AJ, 122, 565
Sault R.J., Teuben P.J. Wright, M C H., 1995, PASP Conf. S
Sault R.J., Killeen N.E.B., 1999, Miriad Users's Manual, http://www.atnf.csiro.au/computing/software/miriad
Sion E.M., Fritz M.L., McMullin J.P., Lallo, M.D. 1988, AJ, 96, 251
Smith R.J., Croom S.M., Boyle B.J., Shanks T., Miller L., Loaring N.S. 2002, MNRAS, submitted (Paper III)
Stickel M., Padovani P., Urry C.M., Fried J.W., Kuhr H., 1991, ApJ, 374, 431
Stocke, J.T., Morris, S L., Gioia, I, Maccacaro, T., Schild, R. E., Wolter, A., 1990, ApJ, 348, 141
Urry C.M., Padovani P., 1995, PASP 107, 803
Voges W. et al., 1999, A&A, 349, 389
Wolter A., Caccianiga A., Della Ceca R., Maccacaro,T., 1994, ApJ, 433, 29
Wesemael, F., Greenstein, J.L., Liebert, J., Lamontagne, R., Fontaine, G., Bergeron, P., Glaspey, J.W., 1993, PASP, 105, 761
White R.L.,Becker R.H., Helfand D.J., Gregg M.D., 1997, ApJ, 475, 479

APPENDIX A: 2DF SPECTRA

Figure A1. 2dF spectra for all the objects in the 2BL sample, including repeat observations. Objects with repeat observations are indicated by an a, b or c after the object name, in descending order of SNR. The SNR of each spectrum and the object's b_J magnitude is also shown. If an object has a measured redshift (not including lower limits), this is shown together with the positions of spectral features. A circled cross marks the location of telluric sky absorption bands. Straight lines in the spectra indicate the removal of night sky lines

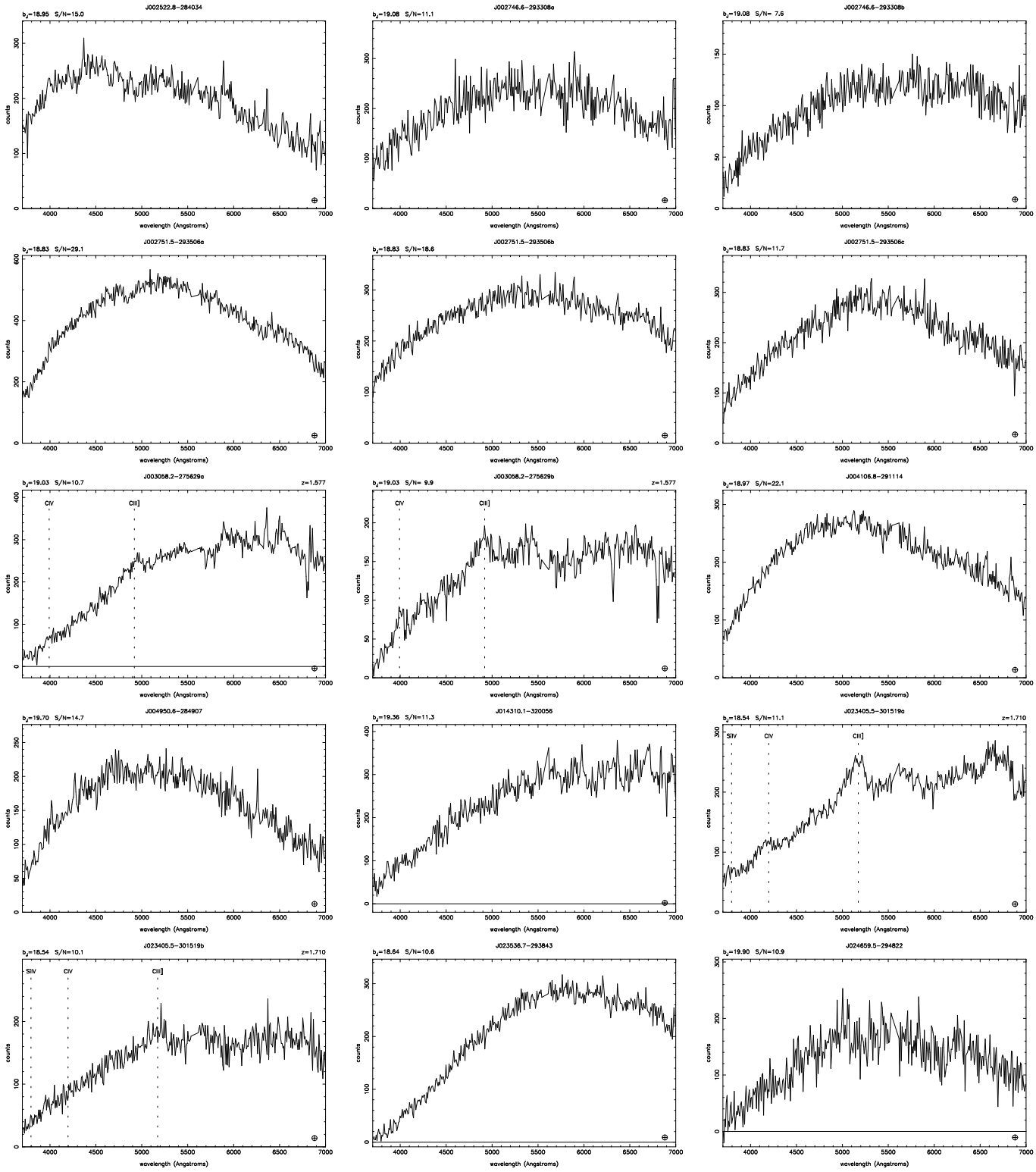

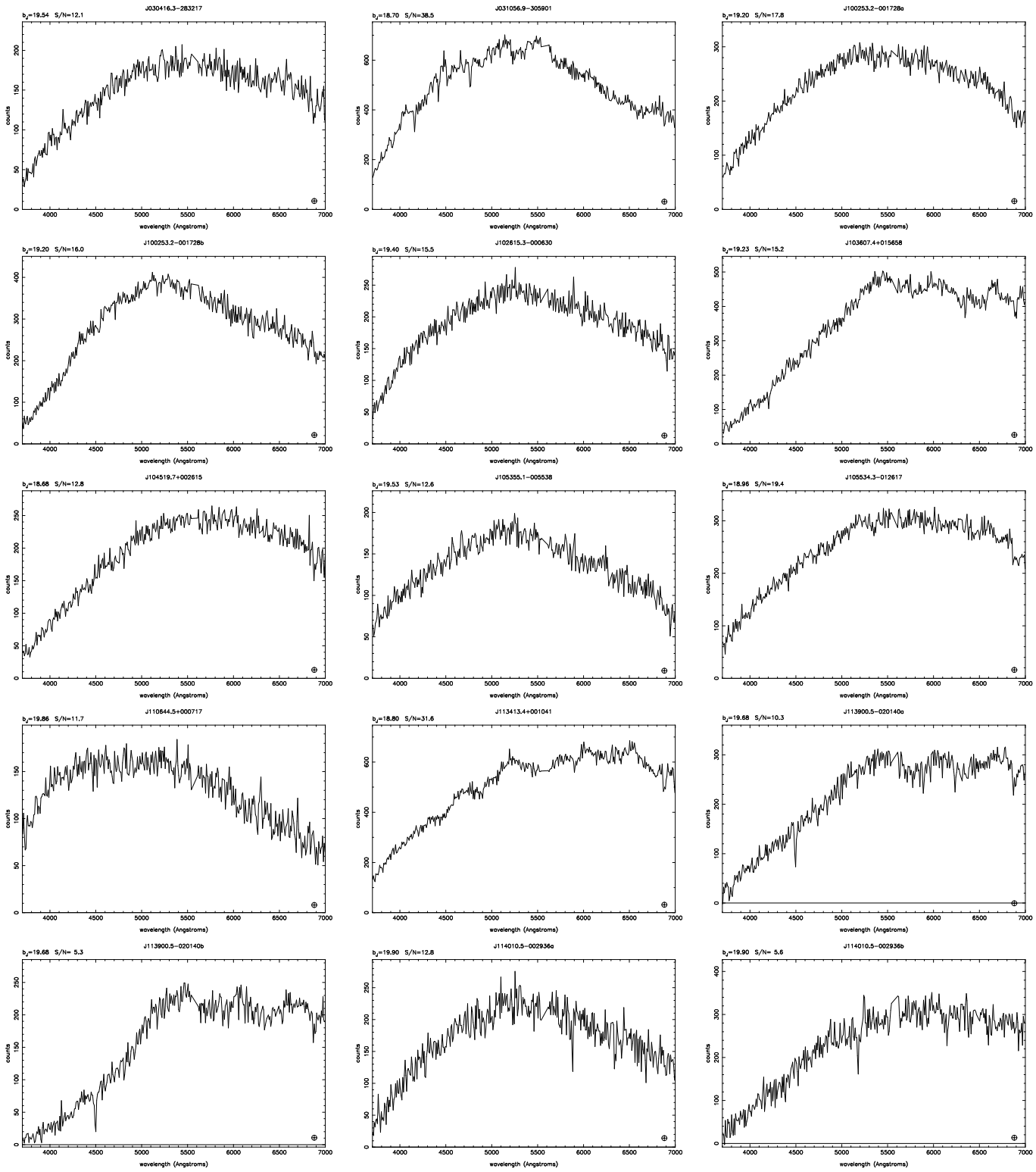
J030416.3−283217
b_J=19.54 S/N=12.1
J031056.9−305901
b_J=18.70 S/N=38.5
J100253.2−001728a
b_J=19.20 S/N=17.8
J100253.2−001728b
b_J=19.20 S/N=16.0
J102615.3−000630
b_J=19.40 S/N=15.5
J103607.4+015658
b_J=19.23 S/N=15.2
J104519.7+002615
b_J=18.68 S/N=12.8
J105355.1−005538
b_J=19.53 S/N=12.6
J105534.3−012617
b_J=18.96 S/N=19.4
J110644.5+000717
b_J=19.86 S/N=11.7
J113413.4+001041
b_J=18.80 S/N=31.6
J113900.5−020140a
b_J=19.68 S/N=10.3
J113900.5−020140b
b_J=19.68 S/N= 5.3
J114010.5−002936a
b_J=19.90 S/N=12.8
J114010.5−002936b
b_J=19.90 S/N= 5.6
counts
wavelength (Angstroms)

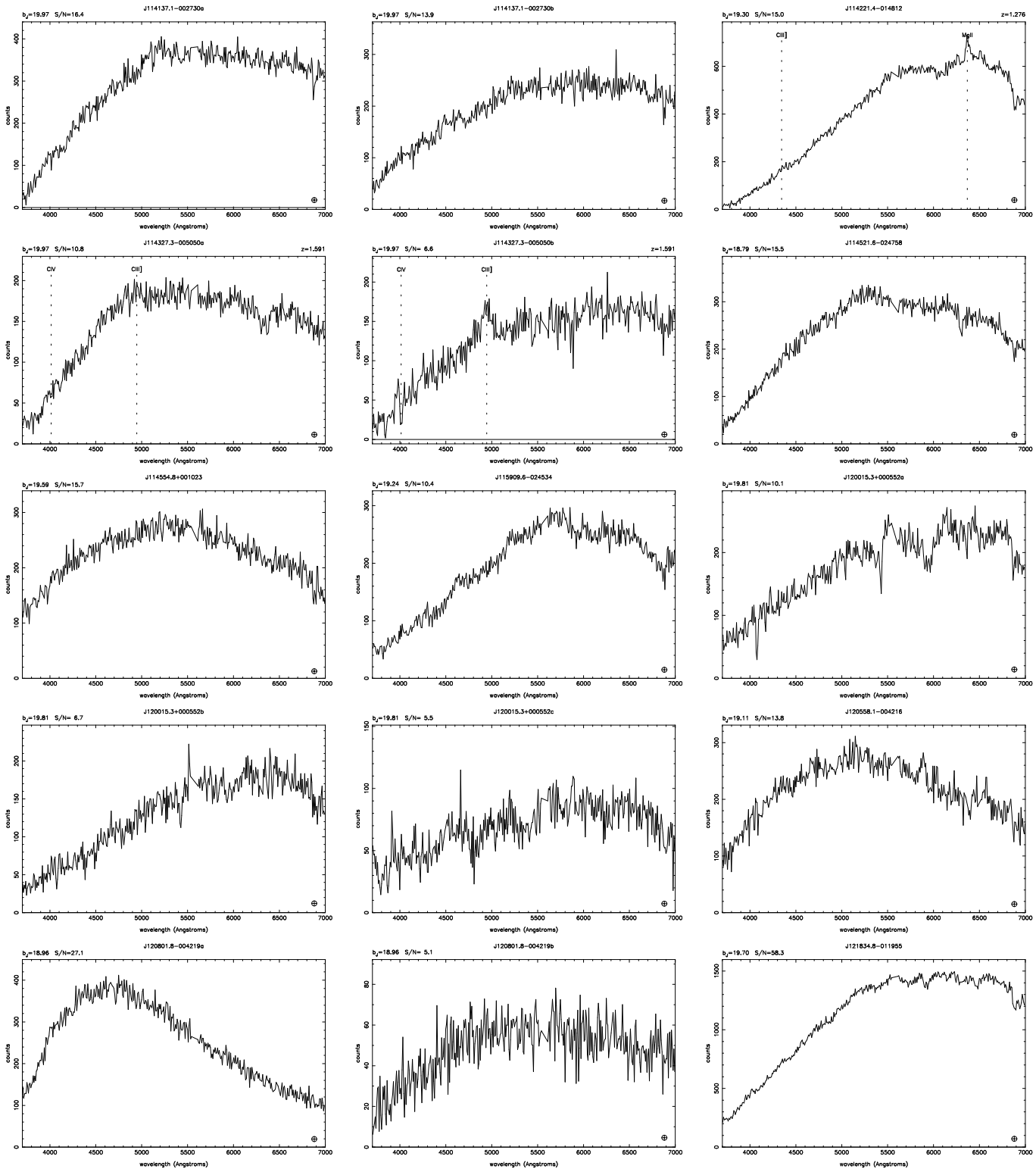
J114137.1−002730a
b_J=19.97 S/N=16.4
J114137.1−002730b
b_J=19.97 S/N=13.9
J114221.4−014812
b_J=19.30 S/N=15.0
z=1.276
CIII]
MgII
J114327.3−005050a
b_J=19.97 S/N=10.8
z=1.591
CIV
CIII]
J114327.3−005050b
b_J=19.97 S/N= 6.6
z=1.591
CIV
CIII]
J114521.6−024758
b_J=18.79 S/N=15.5
J114554.8+001023
b_J=19.59 S/N=15.7
J115909.6−024534
b_J=19.24 S/N=10.4
J120015.3+000552a
b_J=19.81 S/N=10.1
J120015.3+000552b
b_J=19.81 S/N= 6.7
J120015.3+000552c
b_J=19.81 S/N= 5.5
J120558.1−004216
b_J=19.11 S/N=13.8
J120801.8−004219a
b_J=18.96 S/N=27.1
J120801.8−004219b
b_J=18.96 S/N= 5.1
J121834.8−011955
b_J=19.70 S/N=58.3
counts
wavelength (Angstroms)

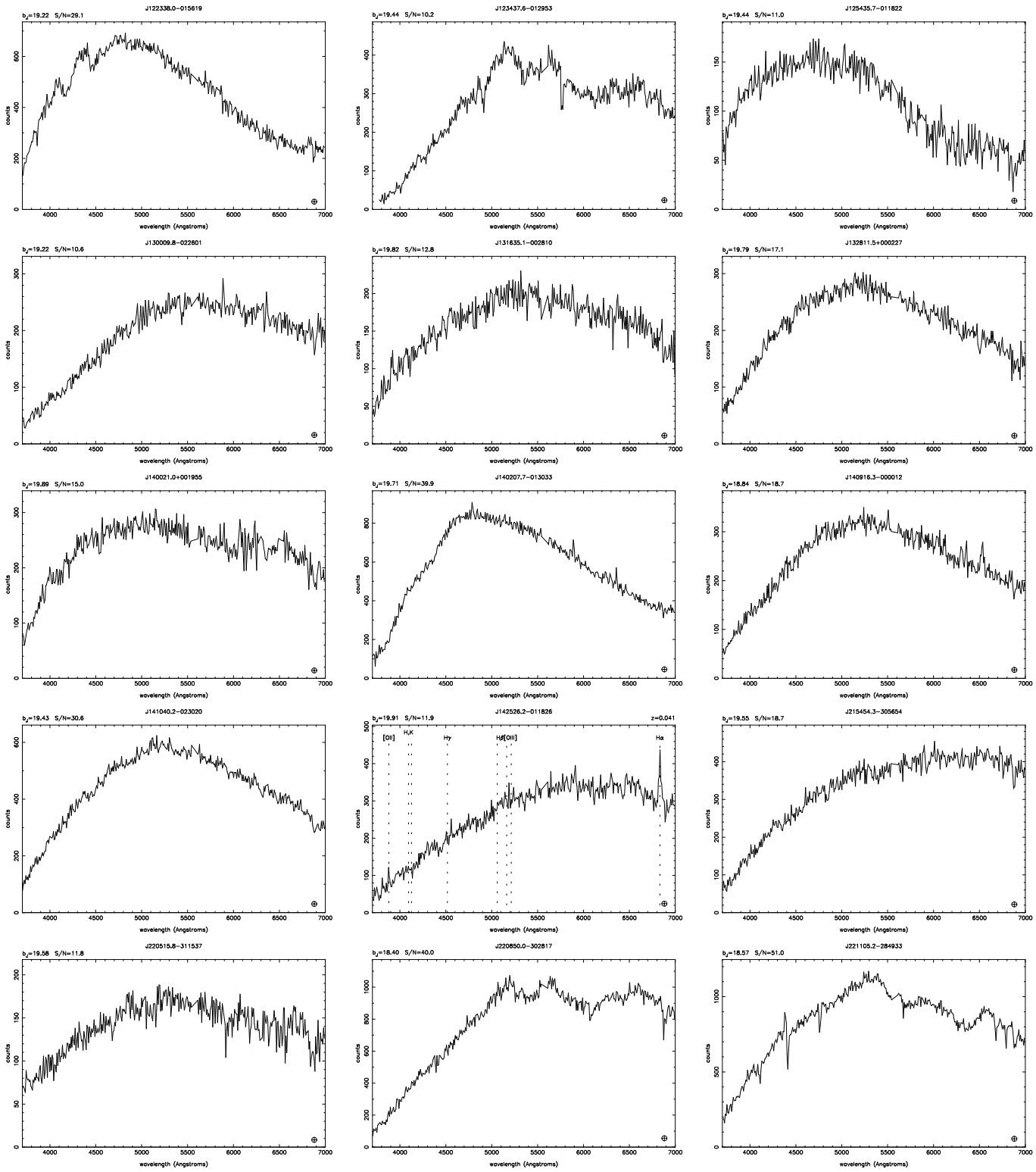
J122338.0−015619
b_J=19.22 S/N=29.1
J123437.6−012953
b_J=19.44 S/N=10.2
J125435.7−011822
b_J=19.44 S/N=11.0
J130009.8−022601
b_J=19.22 S/N=10.6
J131635.1−002810
b_J=19.82 S/N=12.8
J132811.5+000227
b_J=19.79 S/N=17.1
J140021.0+001955
b_J=19.89 S/N=15.0
J140207.7−013033
b_J=19.71 S/N=39.9
J140916.3−000012
b_J=18.84 S/N=18.7
J141040.2−023020
b_J=19.43 S/N=30.6
J142526.2−011826
b_J=19.91 S/N=11.9
z=0.041
[OII]
H,K
Hγ
Hδ[OIII]
Hα
J215454.3−305654
b_J=19.55 S/N=18.7
J220515.8−311537
b_J=19.58 S/N=11.8
J220850.0−302817
b_J=18.40 S/N=40.0
J221105.2−284933
b_J=18.57 S/N=51.0
counts
wavelength (Angstroms)

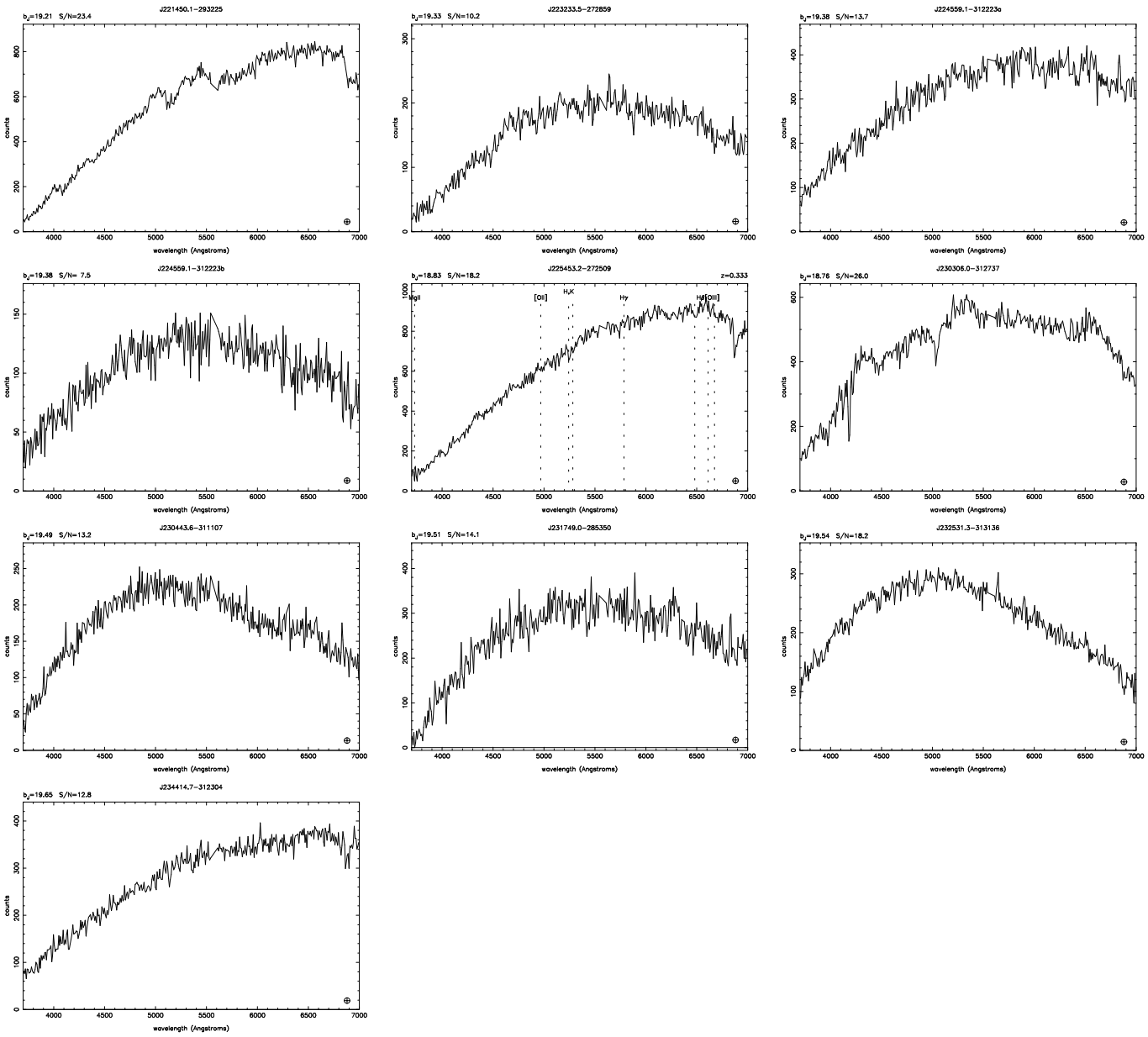
J221450.1−293225
b_J=19.21 S/N=23.4
J223233.5−272859
b_J=19.33 S/N=10.2
J224559.1−312223a
b_J=19.38 S/N=13.7
J224559.1−312223b
b_J=19.38 S/N= 7.5
J225453.2−272509
b_J=18.83 S/N=18.2
z=0.333
MgII
[OII]
HδK
Hγ
Hβ
[OIII]
J230306.0−312737
b_J=18.76 S/N=26.0
J230443.6−311107
b_J=19.49 S/N=13.2
J231749.0−285350
b_J=19.51 S/N=14.1
J232531.3−313136
b_J=19.54 S/N=18.2
J234414.7−312304
b_J=19.65 S/N=12.8
counts
wavelength (Angstroms)